



ISTITUTO NAZIONALE DI RICERCA METROLOGICA Repository Istituzionale

Magnetic Loss Decomposition in Co-Doped Mn-Zn Ferrites

This is the author's accepted version of the contribution published as:

Original

Magnetic Loss Decomposition in Co-Doped Mn-Zn Ferrites / Dobak, Samuel; Beatrice, Cinzia; Fiorillo, Fausto; Tsakaloudi, Vasiliki; Ragusa, Carlo. - In: IEEE MAGNETICS LETTERS. - ISSN 1949-307X. - 10:(2019), pp. 1-5. [10.1109/LMAG.2018.2881108]

Availability:

This version is available at: 11696/60023 since: 2021-01-28T14:40:36Z

Publisher:

IEEE

Published

DOI:10.1109/LMAG.2018.2881108

Terms of use:

This article is made available under terms and conditions as specified in the corresponding bibliographic description in the repository

Publisher copyright

IEEE

© 20XX IEEE. Personal use of this material is permitted. Permission from IEEE must be obtained for all other uses, in any current or future media, including reprinting/republishing this material for advertising or promotional purposes, creating new collective works, for resale or redistribution to servers or lists, or reuse of any copyrighted component of this work in other works

(Article begins on next page)

Magnetic loss decomposition in Co-doped Mn-Zn ferrites.

Samuel Dobák^{1,2}, Cinzia Beatrice^{1*}, Fausto Fiorillo¹, Vasiliki Tsakaloudi³, and Carlo Ragusa⁴¹ *Istituto Nazionale di Ricerca Metrologica-INRIM, 10135 Torino, Italy.*² *Institute of Physics, P.J. Šafárik University, 04154 Košice, Slovakia.*³ *Laboratory of Inorganic Materials, CERTH, Thessaloniki, Greece.*⁴ *Energy Department, Politecnico di Torino, 10129 Torino, Italy.*

Received 1 Apr 2016, revised 15 Apr 2016, accepted 20 Apr 2016, published 1 Jun 2016, current version 15 Jun 2016. (Dates will be inserted by IEEE; "published" is the date the accepted preprint is posted on IEEE Xplore®; "current version" is the date the typeset version is posted on Xplore®).

Abstract— The magnetic properties of sintered Mn-Zn ferrites, Co^{2+} enriched by addition of CoO up to 6000 ppm, have been measured in ring samples on a broad range of peak polarization values (2 mT – 200 mT) and frequencies (dc – 1 GHz). The results have been analyzed by separating the contributions to the magnetization process by the domain walls and the rotations and applying the concept of loss decomposition. By determining value and behavior of the rotational permeability μ_{rot} as a function of the CoO content, we obtain the average effective magnetic anisotropy $\langle K \rangle$ and the related effects on the loss. We thus identify the hysteresis (quasi-static) W_h , rotational W_{rot} , and excess W_{exc} loss components and their dependence on CoO and we verify that the quasi-static loss W_h and the domain wall permeability μ_{dw} consistently pass, together with $\langle K \rangle$, through a minimum value for CoO = 3000 – 4000 ppm. An opposite trend is observed for μ_{rot} . The rotational loss by spin damping $W_{\text{rot, sd}}$ is then calculated by use of the Landau-Lifshitz equation, assuming distributed anisotropy field amplitudes. $W_{\text{rot, sd}}$ covers the experimental loss behavior beyond about 1 MHz. W_{exc} and W_h , both directly generated by the moving domain walls, share the dissipative response of the material at lower frequencies and show similar trends versus CoO content. It is concluded that the modulation of the magnetic anisotropy of Mn-Zn ferrites through Co^{2+} enrichment, leading to maximum magnetic softening for CoO = 3000 – 4000 ppm, can be assessed in terms of separate effects of domain wall motion and moment rotations and the related dissipative properties.

Index Terms—Mn-Zn ferrites, Magnetic losses, Complex permeability, Loss decomposition.

I. INTRODUCTION

The development of low-loss Mn-Zn ferrites, matching the working conditions nowadays posed by the high-speed semiconducting devices used in power electronics and trends towards miniaturization of components, requires understanding of the magnetization process upon a broad range of magnetizing frequencies. Guidelines for optimal preparation methods and composition adjustments [Kalarus 2012] would indeed benefit from a quantitative assessment of the role of structure and composition on magnetic loss and permeability. This is not a simple task, because sintered ferrites are heterogeneous materials, where the magnetization process occurs by admixture of frequency dependent rotations and domain wall (dw) processes, and two different energy dissipation channels, eddy currents and spin damping, operate. Besides the preparation methods and the ensuing structural properties of the sintered material, relevant effects on the magnetic properties are obtained, for example, by operating on the stoichiometry of Fe_2O_3 , that is, on the concentration of the Fe^{2+} ions, which interfere with anisotropy and conductivity [Pascard 1998, Li 2008]. Oxides segregating at the grain boundaries (e.g., CaO, Nb_2O_5 , SiO_2) are routinely added, in order to increase the resistivity [Zaspalis 2002, Wang 2014], while oxides dissolving in the spinel lattice and

releasing cations on the octahedral sites (e.g., TiO_2 , SnO_2 , CoO) can both hinder the hopping mechanism of conductivity and compensate the negative anisotropy of the Fe^{3+} ions [Znidarsic 1995, Fujita 2003, Aiping 2006, Tsakaloudi 2016]. The Co^{2+} cations, in particular, are endowed with nonzero angular moment L_z and are the seat of significant spin-orbit interaction. They can thus provide, even in small concentrations, an anisotropy contribution compensating the negative $\langle 111 \rangle$ anisotropy of the host lattice. This effect, which is understood in terms of the single-ion theory [Darby 1974], is shown to improve the stability of loss and permeability versus temperature and to decrease the loss at room temperature [Fujita 2003, Li 2009, Tsakaloudi 2016, Beatrice 2018]. However, with very low values of the magnetocrystalline energy, additional anisotropy contributions (e.g., induced by field annealing or by magnetostrictive and magnetostatic effects) emerge. Looking, in particular, at the mesoscopic scale of the material and at the grain-to-grain crystallographic discontinuities, we can identify a stochastic distribution of the internal demagnetizing fields at the grain boundaries (i.e. the local dipolar anisotropy), and a corresponding grain-to-grain distribution of the resulting effective anisotropy field H_k . A spectrum of ferromagnetic resonance frequencies and the related dissipation effects are correspondingly expected.

Corresponding author: F. A. Author (f.author@nist.gov). If some authors contributed equally, write here, "F. A. Author and S. B. Author contributed equally."

IEEE Magnetics Letters discourages courtesy authorship; please use the Acknowledgment section to thank your colleagues for routine contributions. Digital Object Identifier: 10.1109/LMAG.XXXX.XXXXXXX (inserted by IEEE).

The phenomenology of anisotropy compensation and its effect on loss and initial permeability is, regarding in particular the role of the Co^{2+} cations, qualitatively known, but quantitatively unexplained [Giles 1976, Fujita 2003, Li 2009]. In fact, restricted frequency and peak polarization ranges are typically explored in the literature, while little physical analysis is provided. When this is attempted, inconsistent conclusions are often drawn. For example, the anisotropy constant K calculated using the Globus' model of coercivity in undoped and Co-doped Mn-Zn ferrites [Fujita 2003] results in too large a center resonance frequency f_0 and too low rotational permeability $\mu_{\text{rot,DC}}$ (typically by a factor 4 – 5). Such limitations are overcome in this work.

We have introduced in previous papers [Beatrice 2017, Beatrice 2018] a quantitative approach to the broadband (dc – 1 GHz) magnetic behavior of Co-doped soft ferrites. It is based on the following main features: 1) Energy loss W and complex permeability $\mu = \mu' - j\mu''$ are simultaneously measured upon the whole broad frequency range. The real μ' and imaginary μ'' permeability components are obtained from the elliptic hysteresis loop of same area W , peak polarization J_p , and peak field H_p as the measured loop, according to the equation

$$W = \pi J_p^2 \frac{\mu''}{\mu'^2 + \mu''^2} = \pi H_p^2 \mu'' \quad [\text{J/m}^3] \quad (1)$$

2) The rotational contributions $\mu'_{\text{rot}}(f)$ and $\mu''_{\text{rot}}(f)$ are experimentally extracted from the measured permeability. The related procedure is discussed in [Beatrice 2017]. $\mu'_{\text{rot}}(f)$ and $\mu''_{\text{rot}}(f)$ are separated from the dw contributions ($\mu'_{\text{dw}}(f)$, $\mu''_{\text{dw}}(f)$) by recognizing, in particular, that the dc hysteresis loss (that is μ''_{DC}) is exclusively generated by the dw motion and that $\mu'_{\text{rot}}(f)$ and $\mu''_{\text{rot}}(f)$ are independent of J_p up to about $J_p = 0.2J_s$, where J_s is the saturation polarization. 3) The so extracted value $\mu'_{\text{rot,DC}}$ permits one to estimate the average effective anisotropy $\langle K \rangle$. In fact, by assuming an isotropic distribution of easy axes, taking into account that for small angle rotations around an easy direction associated with the anisotropy $\langle K \rangle$, making an angle θ with the applied field, the susceptibility is

$$\chi_{\text{rot}} = \frac{J_s^2}{2\mu_0 \langle K \rangle} \cdot \sin^2(\theta), \quad (2)$$

we obtain, after averaging over the half space

$$\mu_{\text{rot,DC}} = 1 + \frac{J_s^2}{3\mu_0 \langle K \rangle} \quad (3)$$

4) We apply the concept of loss separation and write the total measured loss at given J_p value as $W(f) = W_h + W_{\text{exc}}(f) + W_{\text{rot}}(f)$, where the hysteresis ($f \rightarrow 0$) W_h and the excess $W_{\text{exc}}(f)$ components are associated with the motion of the dws. $W_{\text{rot}}(f) = W_{\text{rot,eddy}}(f) + W_{\text{rot,sd}}(f)$, generated by the rotation of the magnetization, includes an eddy current (classical loss) and a spin damping contribution. It has been shown that the loss separation concept, originally demonstrated and quantitatively formulated for conducting materials with the Statistical Theory of Losses (STL) [Bertotti 1998], can be extended to non-conducting materials [Ferrara 2018], thanks to the universal character of the equation of motion of a dw in a viscous medium [Dillon 1959]. $W_{\text{rot,eddy}}(f)$ can be calculated as discussed in [Fiorillo 2014], but it can be usually disregarded in sufficiently thin samples (below ~ 2 mm). 5) Thanks to the knowledge of $\langle K \rangle$, that is, of the average value H_k of the effective anisotropy field, $\mu'_{\text{rot}}(f)$ and $\mu''_{\text{rot}}(f)$ can be theoretically predicted as solutions of the Landau-Lifshitz equation and, as discussed in the following, $W_{\text{rot,sd}}(f)$ is eventually obtained through (1) and the full loss separation is eventually carried out.

TABLE 1. Physical parameters of the Co-doped Mn-Zn sintered ferrites. $\langle s \rangle \equiv$ average grain size; $\delta \equiv$ density; $\rho_{\text{dc}} \equiv$ dc resistivity; $J_s \equiv$ saturation polarization. The investigated ring samples have outside diameter 14.15–14.44 mm, inside diameter 9.15 – 8.86 mm, thickness 4.55 – 5.02 mm.

CoO (ppm)	$\langle s \rangle$ (μm)	δ (kg/m^3)	ρ_{dc} ($\Omega\text{ m}$)	J_s (T)
0	10.8	4920	4.42	0.540
1000	10.7	4980	5.08	0.534
2000	11.9	4980	5.39	0.529
3000	12.2	5010	5.52	0.524
4000	13.1	4980	5.66	0.522
5000	10.8	5010	5.9	0.532
6000	11.1	5040	6.1	0.536

In this paper, we quantitatively discuss the role of Co doping on the permeability and energy loss behaviors of Mn-Zn sintered ferrites by resorting to the previously introduced permeability and loss decomposition methods. The loss components W_h , W_{exc} , and W_{rot} are all shown to be affected by the presence of the Co^{2+} ions and the related anisotropy effects. W_h and W_{exc} are found, in particular, to pass through a minimum value for $\text{CoO} = 3000 - 4000$ ppm, concurrent with maximum value of the rotational permeability and minimum effective anisotropy.

II. ROTATIONAL AND DOMAIN WALL PERMEABILITY, ANISOTROPY, HYSTERESIS LOSS

The low anisotropy of Mn-Zn ferrites is conducive to a magnetization process, taking place by a combination of rotations and dw displacements. The localized dissipation mechanisms associated with the motion of the dws are responsible for W_h and W_{exc} , while the coarse scale of the rotations lumps the related energy loss W_{rot} into a classical scenario [Bertotti 1998]. Both eddy currents and direct release of energy of the precessing spins to the lattice (spin damping) can operate in Mn-Zn ferrites and, as stressed before, a same interpretative framework based on the STL can be adopted. We have measured energy loss and hysteresis loop by means of a calibrated wattmeter-hysteresisgraph at different J_p values up to 10 MHz in Co-doped Mn-Zn ring samples of base composition $\text{Mn}_{0.821}\text{Zn}_{0.179}\text{Fe}_2\text{O}_4$. μ' and μ'' are calculated from the measured $W(f)$ using (1). They are instead directly measured, typically from 1 MHz to 1 GHz, using a shorted line and a Vector Network Analyzer (Agilent 8753A). We use in this case (1) to calculate W . These two measuring methods, their possible limitations, and the employed apparatus are discussed in detail in previous papers [Fiorillo 2010, Caprile 2012, Fiorillo 2015]. The sintered ring samples were prepared starting from pure raw materials and the prefired powders were Co-doped by adding CoO in quantities varying from 0 to 6000 ppm, besides fixed amounts of CaO and Nb_2O_5 . A detailed description of the processing steps is given in [Tsakaloudi 2016] [Beatrice 2018], while the characterization of the structural and electrical properties of the final samples is reported in [Beatrice 2018]. A few basic physical parameters are summarized in Table 1. The measured hysteresis loops show that (1) is a good approximation up to about $J_p = 0.4J_s$. The question is then posed on the assumptions regarding the type of response (resonance vs. relaxation) by the moving dws and the spins rotating inside the domains [Tsutaoka 2003].

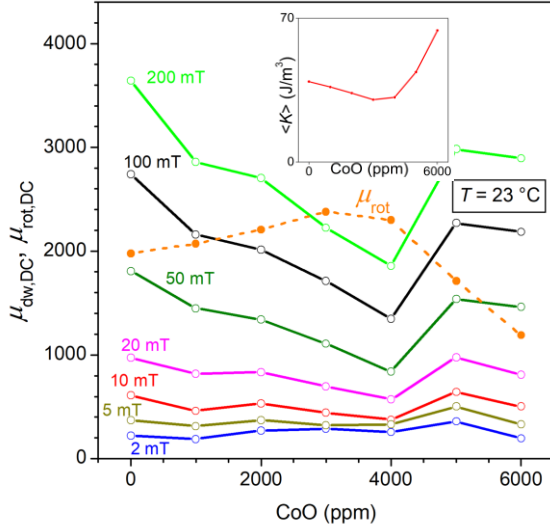


Fig. 1. Rotational (dashed line) $\mu_{rot,DC}$ and dw $\mu_{dw,DC}$ dc permeabilities versus CoO content. $\mu_{rot,DC}$ is obtained according to the decomposition method discussed in [Beatrice 2017]. Magnetic softening occurring at intermediate CoO values is associated with an increased role of the rotations with respect to the dw displacements. The inset shows the correspondingly calculated behavior of the effective average anisotropy $\langle K \rangle$.

As previously stressed, we can separately calculate, following the approach discussed in [Beatrice 2017], μ'_{dw} , μ'_{rot} , μ''_{dw} , and μ''_{rot} from the measured permeability, under the assumption $\mu = \mu' - j\mu'' = (\mu'_{dw} + \mu'_{rot}) - j(\mu''_{dw} + \mu''_{rot})$. This permits us to show, for example, the relaxation character of $\mu_{dw}(f, J_p)$, and the resonant behavior of $\mu_{rot}(f)$ [Beatrice 2017]. An overall picture of the dependence on CoO of the DC rotational and dw permeabilities is provided in Fig. 1. To note the prominent role of $\mu_{rot,DC}$ at the lowest J_p values and the opposite trends of $\mu_{rot,DC}$ and $\mu_{dw,DC}$ vs. CoO. The average effective anisotropy $\langle K \rangle$, calculated with (3), is thus found to pass through a broad minimum for CoO = 3000 – 4000 ppm (inset in Fig. 1), where it attains a value around 30 J/m³, and increases rapidly with increasing CoO, up to 64 J/m³ for CoO = 6000 ppm. To note the simultaneous decrease of hysteresis loss (Fig. 2) and dw permeability with CoO, up to CoO = 4000 ppm. With decreasing $\langle K \rangle$, rotations cover an increasing share of the magnetization reversal with respect to the irreversible dw displacements. The area of the dc loop (inset in Fig. 2) $W_h(J_p) = \lim_{f \rightarrow 0} W(J_p, f)$ is correspondingly affected.

As a first step of the loss analysis, we show that the dependence of $W_h(J_p)$ on Co doping can be to good extent predicted. By posing in fact $W_h(J_p) \cong 4H_c J_{p,dw}$, where H_c is the coercive field and $J_{p,dw} = J_p \cdot \mu_{dw,DC} / (\mu_{dw,DC} + \mu_{rot,DC})$ is the contribution by the dw to J_p , and by considering the inverse dependence of H_c on the average grain size $\langle s \rangle$ [Herzer 1997], a law expected to be valid for $\langle s \rangle$ larger than a few hundred nanometers [Hajalilou 2015], we get

$$W_h \cong 4c_0 \frac{\sqrt{\langle K \rangle}}{\langle s \rangle J_s} \cdot \frac{\mu_{dw,DC}}{\mu_{dw,DC} + \mu_{rot,DC}} J_p, \quad (4)$$

with c_0 a proportionality constant, and $\langle s \rangle$ and J_s given in Table 1. Substantial agreement between the approximate prediction given by (4) and the experimental behaviors of W_h versus CoO is observed. In the following step, the dynamic loss is analyzed and the whole quantitative assessment of $W(f)$ is obtained.

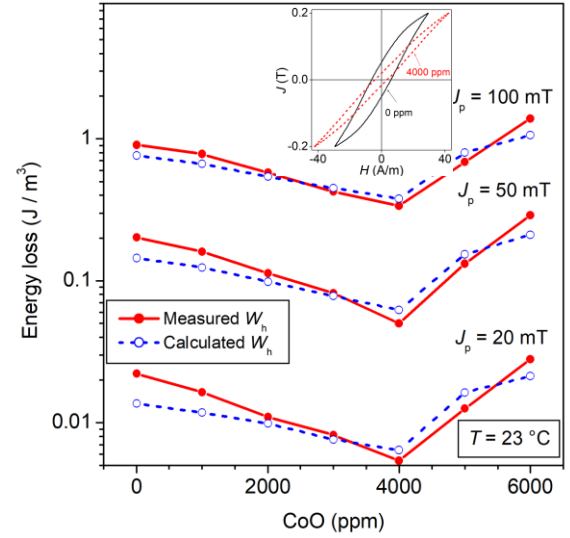


Fig. 2. Quasi-static energy loss $W_h(J_p)$ measured versus the CoO content at three different J_p values and its prediction using (4). The dc hysteresis loops shown in the inset put in evidence that softening by CoO addition takes place by simultaneous decrease of coercive field and irreversible permeability.

III. ENERGY LOSS VERSUS FREQUENCY AND ITS DECOMPOSITION

The benefit of decreased anisotropy by Co doping is apparent in the broadband behavior of the energy loss $W(f)$, shown in Fig. 3 for two different J_p values. $W(f)$ attains, at all frequencies, minimum value in the 4000 ppm CoO sample. It is understood by (4) and Figs. 1 and 2 how and why $W_h(J_p)$ is affected by the $\langle K \rangle$ value. But it is also possible to provide an overall picture of the dynamic contribution to the losses, that is, to identify $W_{exc}(J_p, f)$, which is directly related to the dissipation by the moving dw, and $W_{rot}(J_p, f)$, the term ensuing from the rotation of the moments within the domains and the related resonant effects. Having singled out $W_h(J_p)$, we focus on the dynamic loss by remarking that the concept of excess loss applies whatever the dissipation mechanism, eddy currents or spin damping. As previously remarked, the equation describing the damped motion of a dw, the starting point of the quantitative approach to the excess losses by the STL [Bertotti 1998], is in fact the same in conducting and insulating materials, but for the involved damping coefficient [Dillon 1959]. That an excess loss contribution should emerge in ferrites also follows from the prediction of $W_{rot}(J_p, f)$, which fully covers the dynamic loss only beyond a few MHz, following the complete relaxation of the domain wall processes (i.e. of μ_{dw}). $W_{exc}(J_p, f)$ and $W_{rot}(J_p, f) = W_{rot,eddy}(J_p, f) + W_{rot,sd}(J_p, f)$ include both eddy current and spin damping contributions. $W_{exc,eddy}(J_p, f)$ is negligible in standard Mn-Zn ferrites [Fiorillo 2014]. $W_{rot,eddy}(J_p, f)$ can instead be appreciated only in sufficiently thick specimens, as shown in Fig. 4 for 5.02 mm thick 4000 ppm CoO ring samples. The contribution $W_{rot,eddy}(J_p, f)$, appearing only beyond a few MHz, is here shown to become negligible upon sample thinning down to 1.30 mm.

We are thus left to describe the properties of the spin damping contribution $W_{rot,sd}(J_p, f)$. This amounts to find the frequency

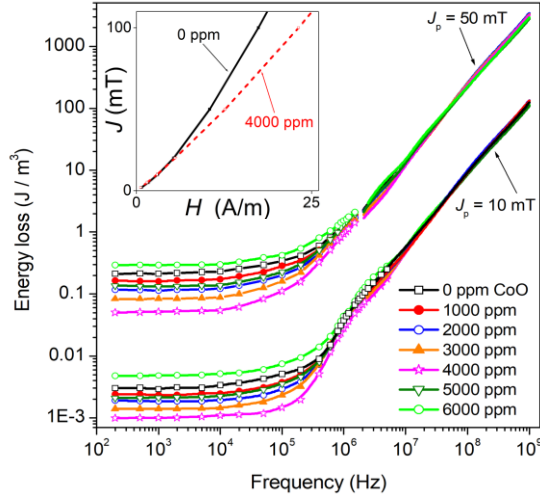


Fig. 3. Energy loss versus frequency at $J_p = 10$ mT and $J_p = 50$ mT up to CoO = 6000 ppm. Symbols and continuous lines refer to fluxmetric and VNA measurements, respectively. The 4000 ppm CoO sample exhibits the lowest loss figure up to a few MHz, where all curves tend to coalesce. Inset: normal (J , H) dc curves within the Rayleigh region for CoO = 0 and CoO = 4000 ppm.

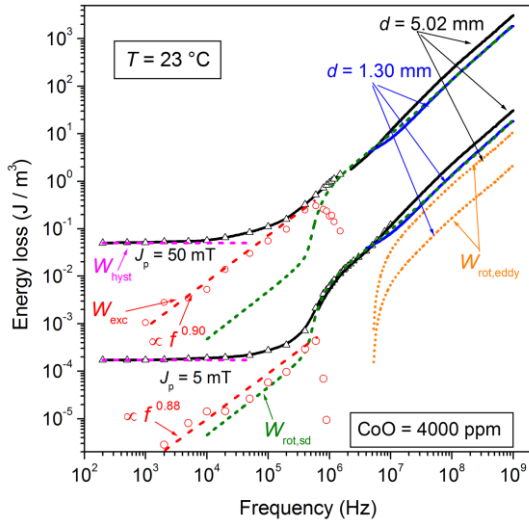


Fig. 4. Decomposition at two J_p values of the energy loss $W(f)$ in a Co-doped ring sample, before and after thickness reduction (from 5.02 mm to 1.30 mm, thick solid lines). An eddy current contribution $W_{rot,eddy}$ is appreciated in the thicker sample above a few MHz (dotted lines for $J_p = 5$ mT). The predicted spin damping rotational loss $W_{rot,sd}(f)$ is shown by the short-dash lines. $W_{exc}(f)$ (circles) is obtained by subtracting $W_{rot,sd}(f)$ and W_{hyst} from $W(f)$. It exhibits a power law $W_{exc}(f) \propto f^p$, with $p \sim 0.9$ and drops on approaching the MHz range (dw relaxation).

dependent constitutive equation of the material for the rotational processes, which, under the assumption of low J_p values, is expressed in terms of complex permeability, solution of the Landau-Lifshitz equation. For a polycrystalline ferrite sample, the real $\chi'_{rot}(H_k, f)$ and imaginary $\chi''_{rot}(H_k, f)$ susceptibilities for a given $H_k = 2K/J_s$, value are averaged over a uniform distribution of orientations of the easy axes and a lognormal distribution $g(H_k)$ for the amplitude of H_k (i.e. of ferromagnetic resonance frequencies). The latter is a typical choice for the distributed local coercive fields in Preisach modeling [Cornejo 1997]. We have [Ferrara 2018]

$$\langle \chi'_{rot}(f) \rangle = \frac{2}{3} \int_0^\infty g(H_k) \chi'_{rot}\left(f, H_k, \frac{\pi}{2}\right) dH_{k,eff}, \quad (5)$$

where $\chi'_{rot}(f, H_{k,eff}, \frac{\pi}{2})$ is the solution at the frequency f of the Landau-Lifshitz equation for anisotropy field of strength H_k orthogonal to the exciting AC field. The same is for $\langle \chi''_{rot}(f) \rangle$.

The lognormal distribution function for $g(H_k)$ is expressed as

$$\langle g(H_k) \rangle = \frac{1}{\sqrt{2\pi}\sigma H_k} \cdot \exp\left[-\frac{(\ln(H_k)-h)^2}{2\sigma^2}\right], \quad (6)$$

where $h = \langle \ln(H_k) \rangle$ and σ is the standard deviation of $\ln(H_k)$. As discussed in [Beatrice 2017] this distribution is assumed to widen upon and beyond the resonance region, because of increasing internal demagnetizing fields (i.e. increasing effective local anisotropies). The rotational loss $W_{rot,sd}(J_p, f)$ is obtained from the calculated $\mu'_{rot}(f) = 1 + \langle \chi'_{rot}(f) \rangle$ and $\mu''_{rot}(f) = \langle \chi''_{rot}(f) \rangle$ using (1). It is shown for the 1.30 mm thick 4000 ppm CoO ferrite in Fig. 4 (short-dash lines fitting the lower branch of the curve). By subtracting $W_{rot,sd}(J_p, f)$ and $W_h(J_p)$ from the total loss $W(J_p, f)$, we obtain the excess loss $W_{exc}(J_p, f)$ (open symbols). $W_{exc}(J_p, f)$ follows an f^p power law, with $p \sim 0.9$ and drops in the MHz region, concurrent with the relaxation of the dw processes. Fig. 5 shows that $W_{exc}(J_p, f)$ follows the same trend as $W_h(J_p)$ and exhibits minimum value for CoO = 4000 ppm, as expected from its theoretical formulation [Ferrara 2018].

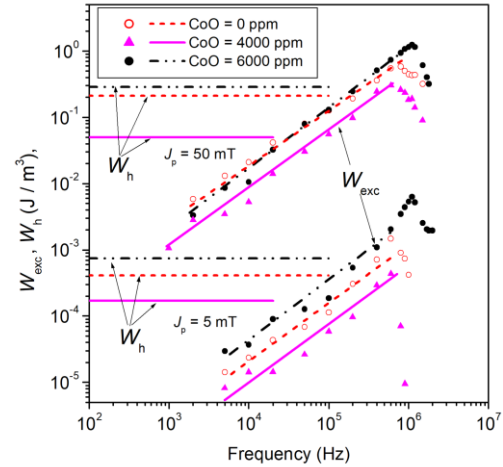


Fig. 5. The excess loss $W_{exc}(f)$ and the hysteresis loss W_h behave in a correlated fashion and attain minimum value for CoO = 4000 ppm. This is expected on theoretical grounds [Ferrara 2018].

IV. CONCLUSION

The effective magnetic anisotropy in Co-doped Mn-Zn ferrites, obtained by calculated behavior of the rotational permeability, attains minimum value for added CoO = 3000 - 4000 ppm. The dw permeability, quasi-static loss and excess loss are correspondingly minimized. It is shown that the loss decomposition can be applied to these semi-insulating materials, independent of the specific dissipation mechanism (eddy currents vs. spin damping). The high frequency response, in particular, is fully described by use of the complex rotational permeability, solution of the Landau-Lifshitz equation, which plays the role of rate-dependent magnetic constitutive equation. The moving dw's provide instead most of the loss contributions below about 1 MHz, their viscous motion being affected by doping to quite larger extent than the magnetization rotations.

ACKNOWLEDGMENT

This work was performed in the context of the Agreement of Scientific and Technological Cooperation between INRIM and CERTH regarding the study of soft ferrites. One of the authors (S. Dobák) acknowledges support from the project KVARĀ (ITMS 26110230084), financed through the European Social Fund and by the project VEGA 1/0330/15 of the Scientific Grant Agency of the Ministry of Education, Science, Research and Sport of the Slovak Republic and the Slovak Academy of Science.

REFERENCES

- Aiping H, Huahui H, Zekun F (2006), "Effects of SnO₂ addition on the magnetic properties of manganese zinc ferrites," *J. Magn. Magn. Mater.*, vol. 301, pp. 331-335, doi: 10.1016/j.jmmm.2005.07.011.
- Beatrice C, Tsakaloudi V, Dobák S, Zaspalis V, Fiorillo F (2017), "Magnetic losses versus sintering treatment in Mn-Zn ferrites," *J. Magn. Magn. Mater.*, vol. 429, pp. 129-137, doi: 10.1016/j.jmmm.2016.12.121.
- Beatrice C, Dobák S, Tsakaloudi V, Ragusa C, Fiorillo F, Martino L, Zaspalis V (2018), "Magnetic loss, permeability, and anisotropy compensation in CoO-doped Mn-Zn ferrites," *AIP Adv.*, vol. 8, 047803, doi: 10.1063/1.4993718.
- Bertotti G (1998), *Hysteresis in Magnetic Materials*, San Diego: Academic Press, p. 391.
- Caprile, A, Coisson M, Fiorillo F, Kabos P, Manu O M, Olivetti E S, Olariu M A, Pasquale M, Scarlatache V A (2012), "Microwave behavior of polymer bonded iron oxide nanoparticles," *IEEE Trans. Magn.*, vol. 48, pp. 3394-3397, doi: 10.1109/TMAG.2012.2200462.
- Cornejo D R, Lo Bue M, Basso V, Bertotti G, Missell F P (1997), "Moving Preisach model analysis of nanocrystalline SmFeCo," *J. Appl. Phys.*, vol. 81, pp. 5588-5590, doi: 10.1063/1.364608.
- Darby M I, Isaac E D (1974), "Magnetocrystalline anisotropy of ferro- and ferrimagnetics," *IEEE Trans. Magn.*, vol. 10, pp. 259-304, doi: 10.1109/TMAG.1974.1058331.
- Dillon J F, Earl H E (1959), "Domain wall motion and ferromagnetic resonance in a manganese ferrite," *J. Appl. Phys.*, vol. 30, pp. 202-213, doi: 10.1063/1.1735134.
- Ferrara E, Fiorillo F, Beatrice C, Dobák S, Ragusa C, Magni A, Appino C (2018), "Characterization and assessment of the wideband magnetic properties of nanocrystalline alloys and soft ferrites," *J. Mater. Res.*, vol. 33, pp. 2120-2137, doi: 10.1557/jmr.2018.275.
- Fiorillo F (2010), "Measurements of magnetic materials," *Metrologia*, vol. 47 pp. S114-S142, doi: 10.1088/0026-1394/47/2/S11.
- Fiorillo F, Beatrice C, Bottauscio O, Carmi E (2014), "Eddy current losses in Mn-Zn ferrites," *IEEE Trans. Magn.*, vol. 50, 6300109, doi: 10.1109/TMAG.2013.2279878.
- Fiorillo F, Beatrice C (2015), "A comprehensive approach to broadband characterization of soft ferrites," *Int. J. Appl. Electromagn. Mech.*, vol. 48, pp. 283 - 294, doi: 10.3233/JAE-152000.
- Fujita A, Gotoh S (2003), "Temperature dependence of core loss in Co-substituted MnZn ferrites," *J. Appl. Phys.*, vol. 93, pp. 7477-7479, doi: 10.1063/1.1557952.
- Giles A D, Westendorp F F (1976), "The effect of cobalt substitution on some properties of manganese zinc ferrites," *J. Phys. D: Appl. Phys.*, vol. 9, pp. 2117-2122, doi: iopscience.iop.org/0022-3727/9/14/020.
- Hajalilou A, Hashim M, Kamari H M, Masoudi M T (2015), "Effects of milling atmosphere and increasing sintering temperature on the magnetic properties of nanocrystalline Ni_{0.36} Zn_{0.64} Fe₂O₄," *J. Nanomater.*, vol. 2015, pp. 1-11, doi: 10.1016/S1567-2719(97)10007-5.
- Herzer G (1997), "Nanocrystalline soft magnetic alloys," in *Handbook of Magnetic Materials*, vol.10, K.H.J. Buschow, Ed., Amsterdam: Elsevier, pp. 415-462, doi: 10.1016/S1567-2719(97)10007-5.
- Kalarus J, Kogias G, Holz D, Zaspalis V (2012), "High permeability-high frequency stable MnZn ferrites," *J. Magn. Magn. Mater.*, vol. 324, pp. 2788-2794, doi.org/10.1016/j.jmmm.2012.04.011.
- Li L (2008), "Influence of Fe₂O₃ stoichiometry on initial permeability and temperature dependence of core loss in MnZn ferrites," *IEEE Trans. Magn.*, vol. 44, pp. 13-16, doi: 10.1109/TMAG.2007.910232.
- Li L, Lan Z, Yu Z, Sun K, Xu Z (2009), "Effects of Co-substitution on wide temperature ranging characteristic of electromagnetic properties in MnZn ferrites," *J. Alloys Comp.*, vol. 476, pp. 755-759, doi: 10.1016/j.jallcom.2008.09.101.
- Pascard H (1998), "Basic concepts for high permeability in soft ferrites," *J. Phys. Fr.*, vol. 8, pp. 377-384, doi: 10.1051/jp4:1998288.
- Stoppels D (1996), "Developments in soft magnetic power ferrites," *J. Magn. Magn. Mater.*, vol. 160, pp. 323-328, doi: 10.1016/0304-8853(96)00216-8.
- Tsakaloudi V, Zaspalis V (2016), "Synthesis of a low loss Mn-Zn ferrite for power applications," *J. Magn. Magn. Mater.*, vol. 400, pp. 307-310, doi: 10.1016/j.jmmm.2015.07.064.
- Tsutaoka T (2003), "Frequency dispersion of complex permeability in Mn-Zn and Ni-Zn spinel ferrites and their composite materials," *J. Appl. Phys.*, vol.93, pp. 2789-2796.
- Wang S, Chiang Y, Hsu Y, Chen C (2014), "Effects of additives on the loss characteristics of Mn-Zn ferrite," *J. Magn. Magn. Mater.*, vol. 365, pp. 119-125, doi: 10.1016/j.jmmm.2014.04.043.
- Zaspalis V T, Antoniadis E, Papazoglou E, Tsakaloudi V, Nalbantian L, Sikilidis C A (2002), "The effect of Nb₂O₅ dopant on the structural and magnetic properties of MnZn ferrites," *J. Magn. Magn. Mater.*, vol. 250, pp. 98-109, doi: 10.1016/S0304-8853(02)00367-0.

Znidarsic A, Lempel M, Drofenik M (1995), "Effect of dopants on the magnetic properties of MnZn ferrites for high frequency power supplies," *IEEE Trans. Magn.*, vol. 31, pp. 950-953, doi: 10.1109/20.364767.